Volumetric Characterization of Hamster Greater Superficial Petrosal and Glossopharyngeal Taste Afferent Terminal Fields

Michelle Jolie Chastain

An Honors Thesis Submitted to the Neuroscience Faculty

Washington and Lee University

May 24, 2005

INTRODUCTION

In developing sensory systems, perinatal changes in afferent activity can influence central organization. The continual turnover of receptor and the corresponding maintenance of appropriate afferent innervation of newly born taste receptor cells has made the taste system an attractive model for the investigation of several aspects of neural development and plasticity. Dynamic in nature, the gustatory system is one of the few sensory systems that constantly undergoes degeneration and regeneration. Taste receptor cells located on the oral, pharyngeal, and laryngeal epithelium experience ongoing degeneration and renewal. In this sense, the gustatory system can be said to recapitulate early neuronal development. During development, immature axons must select the appropriate peripheral and central target in order to establish normal function. This is comparable in the adult taste system, afferents must reselect appropriate taste receptor cells in order to maintain proper taste function. Appropriate synapse formation is presumably driven by interactions between afferent axons and newly born taste receptor cells. Consequently, developmental changes in the afferent taste activity which occur as a consequence of receptor maturation may also influence synaptic organization in the CNS. These modifications occurring in the peripheral gustatory system, especially during development, are perceived and as a result, affect the nature of the synaptic connectivity and arrangement in the brainstem.

In order to study the possibility of developmental changes in structure, a comprehensive understanding of the anatomical organization of the terminal fields in the adult animal must be obtained. While much central gustatory structure has been

described in considerable detail, a more macroscopic characterization of the spatial organization and interrelation of the major taste afferent terminal fields has been overlooked. The present study is a first step toward establishing normative adult data that describe, in quantitative terms, the volumetric and spatial relationship of the greater superficial petrosal (GSP), chorda tympani (CT), and glossopharyngeal (GX) nerves. We provide here a quantitative characterization of the NTS terminal fields of the GSP and GX nerves in the adult hamster as well as regions of overlap between them. To our knowledge, this is the first demonstration of GSP terminal field in this species as well as the first demonstration of simultaneously labeled terminal fields. This thesis begins with an overview of basic gustatory anatomy (peripheral and central) followed by a brief synopsis of the literature regarding the plastic changes that occur in the developing gustatory system.

Peripheral Gustatory Anatomy

The mammalian peripheral taste system is comprised of a highly functionally and anatomically organized set of unique neuroepithelial receptor and support cells and their afferent axons. The basic functional unit of the gustatory system is the taste receptor cell. Morphologically specialized for its function, the taste receptor cell is an elongated neuroepithelial cell with microvillar processes that project from the apical end (or end facing the oral cavity) and sample the environment (Stewart et al., 1997). Receptors for specific tastant molecules are present on these processes, the binding of which results in the transduction, via one of numerous mechanisms, of the chemical signal indicating the detection of that molecule. On the basolateral end, taste receptor cells are innervated by pseudobipolar cranial nerve sensory axons. Taste receptor cells are aggregated in taste

buds and are joined to one another just below the oral epithelium by tight junctional complexes (Stewart et al., 1997). Typically, taste receptor aggregations are called taste buds. These taste buds can exist solitarily or be aggregated within papillae, the organization of which depends on morphology; innervation; and location.

Palatal taste buds are located in the hard palate, the border of the hard and soft palate, and on the soft palate proper. Buds here are ipsilaterally innervated by the greater superficial petrosal nerve (GSP), a branch of the VIIth cranial nerve (St. John et al., 2003). Located on the anterior third of the tongue, fungiform papillae typically contain one to several taste buds whose taste receptor cells are ipsilaterally innervated by the chorda tympani nerve (CT), also a branch of the facial (VIIth) nerve (Stewart et al., 1997). Located more posteriorly and laterally on the tongue, foliate papillae are leaf-shaped trenches, the walls of which contain numerous taste buds whose taste receptor cells are ipsilaterally innervated by the CT (more anterior) and the glossopharyngeal nerve (GL) (more posterior). The third type of lingual papilla, the circumvallate is located on the caudal border of the tongue and is characterized by a semi-circular morphology surrounded by a trench-like depression. Circumvallate papilla taste buds are located along the walls of these trenches and are innervated by the GL (Stewart et al., 1997). It is notable that taste buds located in the central walls of the trench are bilaterally innervated, whereas taste buds on the lateral walls are unilaterally innervated. Finally, approximately 10% of taste buds are located on the laryngeal surface of the epiglottis which are innervated by the super laryngeal nerve (SLN), a branch of the vagus, or Xth cranial nerve (Zigmond et al., pp. 720-721).

Central Gustatory Anatomy

All of the aforementioned primary taste afferent nerves project to the ipsilateral nucleus tractus solitaris (NTS), which extends through the dorsal medulla from the level of entry of the intermediate nerve to the pyramidal decussation (Whitehead & Frank, 1983). Both the GSP and CT terminate in the rostral-most pole of the NTS whereas the GL terminates somewhat more caudally (Smith & Shepard, pp. 722-723). However, there is probable overlap among their terminal fields. The NTS is the first site in the ascending gustatory pathway where processing and relaying of taste information to higher order regions of the CNS takes place. From the NTS the gustatory pathway extends to third-order neurons in the parabrachial nucleus (PbN) of the pons which in turn, project to the ventroposterioemedial nucleus of the thalamus (Smith & Shepard, pp. 722-723). From the thalamus, taste information is transmitted to the gustatory cortex, an area located within the insular cortex region (Smith & Shepard, pp. 722-723). In addition to this pathway, a second pathway projects to several limbic forebrain areas involved in feeding and autonomic control, including the central nucleus of the amygdala, lateral hypothalamus, and the bed nucleus of the stria terminalis (Smith & Shepard, pp. 722-723).

Whitehead (1988) has characterized specific nuclei that reside in the NTS. He subdivided the NTS of the hamster based on the cytoarchitectural criteria such as cell measurement, cell morphology, and neuropil distribution. He identified 10 nuclear subdivisions, each with specific neuronal architecture based on cell size, shape and packing density. A mixture of elongate, stellate and tufted cells characterizes the rostral central subdivision present in the mediolateral plane which indicate its role in the

processing of gustatory and somatosensory information. While the caudal central subdivision contains a similar mixture of cell types, the neurons here are present in all orientations which indicate its role in processing viscerosensory information. The rostral and caudal lateral subdivisions posses primarily small to medium-sized elongate cells in the subnucleus lateral to the solitary tract. The border between these two subdivisions is not well-defined, indicative of a mixture of both gustatory and viscerosensory processing. The medial subdivision is characterized by sparsely dispersed small to medium-sized stellate and tufted cells. The ventral subdivision contains medium to large-sized stellate cells that emit long, moderately branched dendrites in all directions. Although the ventrolateral subdivision possesses similar cell types to its ventral counterpart, the cells found here are much larger. Populated primarily by small stellate neurons, the cells of the dorsal subdivision possess small, thin projections confined to this subdivision proper. The dorsolateral subdivision contains parvidendritic cells, which have small perikarya and long unbranching dendrites. Finally, the laminar subdivision contains predominantly elongate cells oriented parallel to the axis of the subdivision (ventrolateral to dorsomedial).

Earlier, Whitehead and Frank (1983) described the sites of CT and the lingual nerve termination using horseradish peroxidase (HRP) labeling. They found that the CT afferent fibers distribute and terminate to all rostral-caudal levels of the NTS, but terminate most densely in the dorsal half of the NTS at its rostral extreme. The lingual nerve, a branch of the trigeminal nerve which participates in somatosensation of the tongue, terminates heavily in the dorsal third of the spinal nucleus, but has a dense patch of terminations in the lateral NTS between rostral and caudal poles. Similarly, Hamilton

and Norgren (1984) investigated the projections (gustatory and otherwise) of rat cranial nerves V, VII, IX, and X using HRP. Their results indirectly indicate significant overlap between GSP and CT terminal fields primarily is confined to the rostral pole. In addition, they demonstrated that IX had the most spatially extensive NTS dispersion of the primary gustatory nerves. More recently, in different approach to the problem, Travers and Norgren (1995) attempted to map the NTS topographically by recording the neural responses to isolated oral cavity stimuli in the rat NTS. However, their results are unclear, as nearly half of the neurons recorded from responded to two or more areas of stimuli (i.e. taste buds). This result probably relates to complex intracellular connections in addition to the abundance of interneurons found throughout the nucleus (Davis and Jang, 1988). While all of the existing descriptive evidence provides some insight as to the layout of the NTS, the scope of this evidence is limited to the microscopic domain, especially in hamster. A major goal of the current work is to demonstrate simultaneously the spatial relationship between taste afferent terminations.

Peripheral Development and Plasticity

Due to the unique and dynamic sensory environment present during development, a developing sensory system must in turn be modifiable in order establish appropriate synaptic connections. Although not as extensive as in other sensory systems, there exists a sizable literature regarding peripheral gustatory development. Using hemotoxylin and eosin staining techniques, Miller and Smith (1988) demonstrated a complete lack of foliate and vallate taste buds at birth in hamster. However, by postnatal week 5, morphologically mature taste buds were observed, indicating exclusive postnatal development. Belecky (1990) showed that other areas of the oral cavity innervated by

gustatory afferents (palate, epiglottis, and larynx) undergo significant postnatal development in hamster as well. Although the majority (60%) of palatal taste buds are present at birth, they develop a taste pore only during the first 20-30 days postnatally. Since the presence of a patent taste pore is a defining feature of a mature taste bud, this finding suggests that very dynamically changing patterns of afferent activity might be observed in hamster GSP during the first several weeks postnatally. On the other hand, oropharynx taste buds are absent at birth but develop steadily during the first four postnatal months. In striking contrast, Whitehead and Kachele (1994) demonstrated that hamster fungiform taste buds were not only present and of mature morphology at birth, but also the majority of these taste buds displayed open and functional taste pores. Similar to the other sensory systems, there is much evidence supporting the dynamic nature of the peripheral gustatory system.

In addition to protracted anatomical development of the peripheral gustatory system in hamster, there is evidence that taste afferent activity changes dynamically throughout the postnatal period. Hill (1988) described a significant developmental trend in hamster CT responses to salty and sweet stimuli. He found that CT responses to NaCl and LiCl decreased by a factor of approximately 50% during roughly 15-65 days postnatal. On the other hand, CT responses to a variety of saccharide stimuli significantly increased during an overlapping period during the first 30 days postnatal. Other data suggest age-dependent changes in CT sensitivity to bitter stimuli (Stewart, unpublished observations). Together, these findings reveal significant postnatal changes in physiological sensitivity to specific taste stimuli of a single afferent input that are superimposed on the progressive receptor development discussed above. This reveals

additional complexity in the changing patterns of afferent activity that may influence mature central morphology in the hamster taste system.

Central Development and Plasticity

The dynamic nature of the central gustatory system development is comparable to that of other sensory systems. First, the sensory afferents must migrate and establish contact with the appropriate target neuron in the CNS. In terms of the gustatory system, the CT, GSP, and IX must find the appropriate termination location in the NTS. Lasiter (1992) described time course of development of the three primary gustatory afferents in rat, as well as the temporal relationship between the development of afferent terminal fields and the development of projections neurons located postsynaptically. Using single and double fluorescent labeling, Lasiter (1992) shows that afferent terminal fields develop along a rostrocaudal gradient. Specifically, CT and GSP afferents are present in the rostral NTS at postnatal day 1 and develop caudally until day 25. On the other hand, IX afferents do not appear in the NTS until postnatal day 9-10 and continue to develop in the intermediate NTS until day 45. Results also indicate that as the afferent terminal fields develop, they establish synaptic connection with the parabrachial nucleus (PBN), a primary sight of second order processing, approximately postnatal day 45-60. Moreover, evidence suggests if a similar pattern of growth occurs, it may be highly susceptible to the changing peripheral activity patterns in development.

Evidence exists from rat that demonstrates how changes in peripheral input alter the gustatory development in the NTS. Lasiter and Kachele (1990) demonstrated early postnatal damage of rat fungiform receptors resulted in alterations in CT and GSP terminal field morphologies in the NTS. These alterations persisted into adulthood.

Lasiter and Kachele (1990) concluded that the receptor damage eliminated the caudally directed migration of CT/GSP axons to additional projection neurons in the NTS, which normally establish connections with the second order gustatory relay in the parabrachial nucleus. They further hypothesized that this caudally-directed "field migration" depended upon patterns of activity in the afferent population. Lasiter and Diaz (1992) explored this idea by examining the effect of artificial rearing on rat gustatory terminal field development using an intragastric cannula. Again using fluorescent tracing methodology, they found that modified early taste experience produced alterations in development of the gustatory terminal fields in the NTS similar to those found in Laister and Kachele (1990). Given this evidence in the rat as well as the evidence of immense postnatal peripheral development in the hamster, it seems likely the environment present in early development would result in changes in the terminal field features of the NTS.

While the evidence presented is promising, it is important to consider normal developmental plasticity of the central gustatory system is just now beginning to yield to examination. Thus, extending such effort to the developing hamster taste system is especially timely. Moreover, the remarkable peripheral gustatory anatomical and functional changes that occur during postnatal development in hamster make this species a particularly attractive model for the study of central development plasticity. Such an examination will be illuminated by a characterization of the three primary gustatory terminal fields and their spatial relationship to one another. As a first step toward identifying changes in gustatory terminal fields during development, this study aims to characterize volumetrically and spatially characterize two of the three primary gustatory afferent terminal fields, namely GSP and IX, and their spatial relationship to one another.

EXPERIMENTAL METHOD/DESIGN

Animals: Adult (90-130 day old) male hamsters served as subjects. Stock male and female Golden Syrian Hamsters obtained from Harlan (Indianapolis, IN) were bred and the offspring reared in dedicated vivarium space maintained at constant temperature (23° C) and relative humidity (50%) with a light: dark cycle of 14h: 10h.

Surgery and nerve labeling: All surgical procedures were performed under aseptic conditions at the University of Virginia according to protocols approved by that institution's Institutional Animal Care and Use Committee. Animals were anesthetized with ketamine-Domitor (40 mg/kg Dormitor, IM, followed by 75 mg/kg ketamine, IM). Surgical anesthesia was assessed by absence of limb withdrawal in response to toe pinch, and maintained by administration of ketamine (25 mg/kg, IM) as necessary. Body temperature was maintained by placing the animal on circulating water heating pad, and corneal protection was afforded by application of sterile ocular surgical ointment.

Animals were placed into appropriately sized non-traumatic head holders and supinated. Through a midline incision overlying the sternohyoideus, the tympanic bulla was exposed by gentle static retraction of the sternohyoideus, sternomastoideus, and posterior belly of the digastricus, and then opened with a small hole on the ventral aspect. The GSP nerve was exposed and isolated through the temporal bone and cut (Sollars and Hill, 2000). Crystals of lyophilized 3 kD MW detran amine (Molecular Probes) conjugated with tetramethylrodamine and biotin (micro-ruby) were bulk applied to the isolated proximal stump of the GSP. The IX nerve was then isolated medially and dorsally to the bulla and cut. Crystals of dextran-amine conjugated with Cascade Blue

were applied to the proximal sump. Tracer applications were covered with a quick-curing silicone elastomer (Kwik-Cast WPI) to prevent tracer migration. In some GSP single label animals, other 3 kD dextran amine conjugates were used. These included biotinylated dextran amine (typically visualized with streptavidin-Alexa^{488} conjugate as described below), cascade blue-dextran amine, or rhodamine green-dextran amine. All tracers yielded generally similar transport and terminal field labeling.

Tissue Processing: Following 1-4 days survival (modal survival time=3 days), animals were sacrificed by Nembutal oversdose (150mg/kg, IP) and perfused transcardially with Krebs (pH 7.4, 35-37°C) followed by unbuffered 8% paraformaldehyde (pH ~7.2, 35-37°C). Brains were removed and postfixed overnight in 8% paraformaldehyde (pH ~7.2, 35-37°C). Post-fixed brains were blocked and cut into 50μm horizontal sections on a vibratome. Sections were collected into PBS (pH 7.5) and then incubated for 90 minutes at room temperature in a cocktail containing 1:500 rabbit anti-Cascade Blue and streptavidin-Alexa^{546} in 0.1% Triton X-100 in 10mM PBS (pH 7.5) followed by 1:500 goat anti-rabbit Alexa^{488} (all from Molecular Probes). Sections were then rinsed 3x10 min in fresh changes of PBS and then mounted in 1:1 PBS:glycerol between coverslips for confocal visualization. Single labeled specimens were exposed to those reagents necessary for field visualization.

Confocal laser scanning microscopy and planimetry: Coverslip-mounted sections were scanned at 10X on an Olympus Fluoview 300 CLSM. Sections through the entire dorsal-ventral extent of the NTS were examined serially from dorsal to ventral. First, epifluorescent illumination was used to locate fibers of and terminal field of IX, which is located most dorsally in rostral NTS. Once the dorsal most portion of the IX

field is located (usually about 200 μm deep), 3 μm serial sections were made through each 50 μm physical section using appropriate illumination wavelengths (546:GSP and 488 for IX). These confocal image stacks were saved for offline extraction and terminal field area measurements. Terminal field areas of each nerve (including any overlap) were measured in each extracted 3 μm optical section using *StereoInvestigator* (Microbrightfield). This was accomplished by free-hand tracing of terminal field. The overlap measurements were achieved by examining only the tracings of individual terminal fields (GSP and IX) and free-hand tracing the overlapping areas between them. These areas were then multiplied by optical section thickness to render the terminal field volume. In addition, terminal field volumes were broken down into three zones (dorsal, intermediate, and ventral) to assess regional changes in terminal field distribution. For each animal the total number of optical sections containing measurable terminal field were summated and the sum was divided by three to divide the terminal field into thirds (dorsal, intermediate, and ventral).

Statistical Comparisons: All quantitative morphometric data are represented as a mean ± SEM. The comparisons of this morphometric data between fields were evaluated using an independent t-test. The comparisons of volumetric distribution of terminal field volumes within fields were assessed using a one-way ANOVA and Bonferroni post hoc tests were performed where appropriate.

RESULTS

The data presented here were obtained from 8 single-labeled GSP nerves, 3 single-labeled IX nerves and 3 double-labeled GSP/IX preparations. Morphometric data

for each field are based on data pooled from both single and double label preparations, while field overlap data were derived exclusively from double labels.

Figures 1- 2 depict confocal images of dextran-amine conjugate labeled taste nerve terminal fields. Tracer was effectively transported transganglionically in both IX and GSP. *Figure 1* shows the typical labeling of IX terminal field, and *Figure 2* shows the characteristic labeling of GSP terminal field. Individual terminal fields in double-labeled preparations were essentially indistinguishable from single label preparations. *Figure 3* depicts the surgical approach and labeling of GSP in the middle ear. Micro ruby dye can be seen transported anterogradely toward the palatal receptors (*Figure 3B*). Likewise, the proximal stump of the GSP as well as GSP cell bodies in the geniculate ganglion are heavily labeled (*Figures 3C* and *3D*). A high magnification confocal image of the geniculate ganglion clearly shows GSP fibers entering the ganglion retrogradely and exiting the ganglion anterogradely towards the CNS (*Figure 4*)

Morphometry of GSP and IX Terminal Fields

Summary morphometric data are contained in *Table 1*.

IX

Terminal field of IX initially appeared ~200 μm below the dorsal boundary of caudal NTS and extended ~400 μm ventrally. Labeled IXth nerve terminal field was restricted to the rostral pole of NTS with the densest part of the field seen at intermediate levels in the dorsal-ventral extent of the field (*Figure 1*). The IX field appears to have a greater rostrocaudal extent compared to the GSP, although this was not determined here. IX field also has a characteristic "two-clump" distribution: one rostral clump(presumably for taste information) and one more caudal clump (presumably for taste and viscerosensory information). In addition, part of IX field is seen lateral to the solitary

tract, an observation that is absent in GSP. This part of the IX field is possibly associated with oromotor output neurons that may influence the pharyngeal phase of swallowing movements (Travers & Norgren, 1995).

The terminal field start depth was determined by the first physical section that terminal field appeared. Since each section is 50 μm thick, the start depth can be determined by multiplying the number of sections deep by 50 μm. The dorsal-ventral extent was determined by multiplying the number of optical sections containing field by the thickness of an optical section (3 μm). The total volume of IX field was determined by summing the volumes of each optical section. The mean IX terminal field volume was $63.3 \pm 11.9 \times 10^6$ μm^3 (*Figure 8*). The mean IX dorsal-ventral extent was 370.0 ± 46.7 μm (*Figure 7*), and the mean IX start depth was 183.3 ± 42.2 μm (*Figure 6*).

Next, the total number of optical sections containing terminal field was determined for each animal and divided by three to establish dorsal, intermediate, and ventral zones of the terminal field. The volume for each third was expressed as a percentage of the total field volume (*Figure 9*). The mean percentage of IX terminal field volume contained in the dorsal zone was 22.2 ± 1.2 %. The mean percentage contained in the intermediate zone was 50.3 ± 3.2 %, while that contained in the ventral zone was 27.5 ± 3.8 %. ANOVA was used to determine whether terminal field volume was distributed among the 3 field zones in a statistically significant manner. A significant main effect of field zone on terminal field volume percentage was found, ($F(2,17)=25.37$, $p<0.001$). Post hoc Bonferroni tests revealed that the percentage of field volume contained in the dorsal zone of the field volume was significantly less than that in

the intermediate zone volume ($p<0.001$), and that both the dorsal and intermediate zones contained significantly more field volume than the ventral zone ($ps<0.05$) (*Table 1*).

GSP

GSP terminal field initially appeared ~327 μm below the dorsal boundary of caudal NTS and extended ~322 μm ventrally. Most GSP fibers entered the NTS rostrally, especially in the intermediate and ventral portions of the terminal field Labeled GSP terminal field was restricted to the rostral pole of NTS with the densest part of the field seen rostrolaterally, adjacent to the solitary tract. The mean GSP start depth was 327.3 ± 31.9 μm. The mean GSP dorsal-ventral extent was 322.4 ± 49.6 μm. The mean GSP terminal field volume was 34.3 ± 4.6 x 10^6 μm^3.

The mean percentage of GSP terminal field volume contained the dorsal zone was 30.4 ± 2.8 % (*Figure 9*). The mean percentage for the intermediate zone was 47.5 ± 2.1 %, while the the ventral zone was 22.1 ± 1.9%. ANOVA revealed a significant main effect of field component on terminal field volume percentage was found, ($F(2,30)=31.76$, $p<0.001$). Post hoc Bonferroni tests indicated that dorsal zone contained significantly less than the intermediate zone, ($p<0.001$), and that both the dorsal and the intermediate zones contained significantly more field volume than the ventral zone ($ps<0.001$) (*Table 1*).

IX and GSP Field Comparison

To determine any significant differences between IX and GSP morphometric data, independent sample t-test was performed. Although dorsal-ventral extent means were not significantly different, the IX terminal field first appeared a significantly more dorsally

than the GSP, ($t(15) = 2.7$, $p = 0.020$) (*Figure 6*). Similarly, total IX terminal field volume was significantly larger than that of GSP, ($t(15) = -2.7$, $p = 0.015$) (*Figure 8*).

GSP/IX Overlap

The areal overlap of GSP and IX in each optical section of double labeled specimens was measured by tracing areas of overlap between traced GSP and IX fields. The mean start depth of the GSP/IX terminal field overlap is 283.3 ± 16.7 μm deep. The mean dorsal ventral extent of the GSP/IX terminal field overlap is 275.0 ± 32.5 μm. The mean total volume of GSP/IX terminal field overlap is $27.7 \pm 6.5 \times 10^6$ μm^3 (*Figure 8*).

Similar to GSP and IX terminal fields, the total number of optical sections containing GSP/IX field overlap was determined for each animal and divided by three to establish dorsal, intermediate, and ventral zones (*Figure 9*). The dorsal zone contained 24.8 ± 5.0 % of the total field overlap, while the intermediate and ventral zones contained 49.7 ± 0.1 % and 25.4 ± 4.9 %, respectively. When ANOVA was used to determine whether terminal field volume was differentially distributed among the 3 field zones, a significant main effect of field zone on terminal field volume percentage was found, ($F(2,8) = 12.33$, $p = 0.007$). Post hoc Bonferroni tests revealed that the intermediate zone volume was significantly greater than the volumes of both the dorsal and ventral zones ($p < 0.02$), while the dorsal and ventral zone volumes did not differ significantly ($ps > 0.05$) (*Table 1*).

DISCUSSION

Both the IX and GSP terminal fields were intensely labeled by transganglionic transport of 3kD dextran conjugates, allowing for relatively precise terminal volume field measurements. To our knowledge, this is the first anatomical demonstration of GSP terminal field in hamster. Both IX and GSP terminal fields were limited to the rostral portion of the NTS. This is consistent with Whitehead and Frank (1983), who found that the rostral half of the NTS is primarily concerned taste information processing. IX terminal field appears more dorsally than GSP, which extends more ventrally than IX. The total volume of the IX was found to be significantly larger than that of GSP. Volumes of GSP and IX terminal field were distributed predominately in the significantly intermediate third of each field's dorsal-ventral extent. As illustrated in *Figure 10*, the relationship between GSP and IX terminal fields allows for a prediction to be made as to the characteristics of the overlap between the two fields. Since the intermediate and ventral zones of IX spatially overlap spatially with the dorsal and intermediate thirds of GSP, one would expect the highest percentage of GSP/IX terminal field overlap to be found in those areas which spatially overlap.

However, the data from simultaneously visualized IX and GSP fields, which was the first simultaneous demonstration of GSP/IX in hamster, indicate otherwise. For example, the overlap start data is approximately 283 μm, which is 44 μm more dorsal than where the GSP field starts. The discrepancy may be explained by the low of number of subjects in the double labeled data set. Due to time constraints, only 3 double-labels were successfully obtained. Double-labeled terminal fields undoubtedly provide a more

accurate picture of the planimetric specifics of terminal field overlap, since the need to use anatomical landmarks to coregister independent histological samples is obviated. The fact that each terminal field (GSP, IX, and GSP/IX overlap) is present in the same animal reduces the amount of between subjects variance intrinsically present. It will be interesting to see whether with additional observations double label IX/GSP data converge with the single label overlap estimates (*Figure 10*). A lack of convergence would indicate the fundamental shortcoming of attempting to assess anatomical structural overlap from independent histological samples and emphasize the superiority of multiple, simultaneous labeling technique. However, this double label methodology is limited in its scope. In confocal images, overlap sometimes was indicated by a merging of GSP (red) and IX (green) field label emissions to yield yellow. However, overlapping areas usually appeared either green (IX) or red (GSP), suggesting that while fields overlap, they may not converge. Convergent synaptic inputs may be indicated by coincident red and green (yellow on images). However, convergence of taste afferents on common post-synaptic targets will have to ultimately be determined using an ultrastructural approach.

Regardless, the data, despite methodological shortcomings, do indicate a significant degree of overlap between the two fields. Understanding terminal field overlap is essential in order to comprehend the functional processing of taste afferent inputs. Areas of overlap in sensory cortices typically indicate areas of sensory information convergence, and co-processing or integration. Ojima and Takayanagi (2004) indicate that areas of terminal field (in the auditory cortex) that exhibit preferred specific frequency (i.e., isofrequency bands) show areas of overlap and divergence. Their

evidence suggests that areas of overlap between frequency specific terminal fields are consistent with the spectral integration of sound information. Expanding upon this idea, Nakahara et al. (2004) examined the effect of early environmental acoustic exposure on auditory cortex organization. They found that exposure to spectrally and temporally separated lower and higher frequencies radically altered the organization of the auditory cortex. In the gustatory system, specific terminal field components correspond to differential sensitivities for various taste stimuli. Using electrophysiological recordings from CT and GSP, Harada and Smith (1992) demonstrated significantly different sensitivities to sweet and salty stimuli in the two nerves. While both nerves demonstrate sensitivity to both sweet and salty stimuli, they found that GSP is far more sensitive to sweet stimuli than is CT, which is more sensitive to salty. Comparatively speaking, similar evidence exists for the IX nerve. Specifically, in hamster (and most mammals) IX is primarily sensitive to bitter stimuli and secondarily to acidic stimuli (Hanamori et al.,1988). Considering that each nerve possesses a unique range of sensitivities to specific stimuli, any areas of overlap between the taste afferents could indicate an integration site for multiple taste submodalities. Convergence could involve additive sampling (e.g. sweet information from multiple nerves), or polymodal integration (e.g. salty and sweet inputs). Current neurophysiological have not adequately addressed these possibilities. Some areas of overlap between GSP and IX probably represent areas of convergent sensory input and thus, the temporal and a spatial integration of bitter, sour, sweet, and salty taste information.

The terminal field data presented here provide a partial foundation for studies of development of the central gustatory terminal fields. While little research has examined

development in the gustatory CNS, an ample literature exists for other sensory systems, in particular the visual (Hubel and Wiesel, 1970; LeVay et al., 1980), somatosensory (Jacquin et al., 1995; Kaas & Collins, 2003) and nociceptive systems (Fitzgerald and Jennings, 1999). The nociception literature is especially applicable to the gustatory system in that they share similarities in terms of anatomical organization. Fitzgerald and Jennings (1999) described the relationship between Aβ and Aδ somatosensory afferent terminal fields and C fiber nociceptive afferent terminal fields in the spinal cord of developing rat. They noted that Aβ and Aδ fibers appeared in the dorsal grey matter at embryonic day 15 (E15) whereas C fibers do not appear until later E19. They also observed that the perinatal somatotopic organization of these fiber terminal fields is not precise as in the adult, suggesting that plastic changes occur postnatally in response to normal peripheral stimulus input.

In the visual system, alterations in visual cortex ocular dominance columns that occur in response to altered environment during development represent an excellent example of central sensory system plasticity. Hubel and Wiesel (1970) demonstrated that in the developing visual system, monocular neurons are initially, driven by inputs from both eyes. These inputs they directly compete for domination over the same visual cortex neuron. Only later, as a product of synaptic competition, and due to the unequal sensory environment for each eye, are the two imputs segregated into ocular dominance columns (LeVay et al., 1980). However, when one eye is surgically closed early in postnatal development, the layering of the lateral geniculate nucleus as well as the primary visual cortex are disrupted . The area in the visual cortex formerly innervated by axons carrying information from the occupied eye becomes innervated by neurons

carrying information from the open eye. This process is known as an ocular dominance column shift which occurs most notably in layers IVC_{α}. Similar phenomenon occur in binocular neurons in layers IVB and III (Hubel and Wiesel, 1979). The aforementioned systems provide ample evidence of terminal field plasticity, indicating the potential for central gustatory plasticity in response to sensory deprivation.

In rat, GSP and CT axons are observed in the NTS earlier than IX (Laister, 1992). The later arriving IX axons establish a terminal field in areas around the preexisting GSP axons. That is, GSP neurons establish stable synapses first; later developing IX fibers must either colonize unoccupied territory or compete with GSP and CT terminals. In addition, evidence suggests that developing sensory systems (notably the visual system and the neuromuscular junction) establish extensive and inappropriate synaptic connections which are later pared down due to competition from other axons (Mangold & Hill, 2005; Balice-Gordon & Lichtman, 1993) . Mangold and Hill (2005) have provided evidence of this in rat. Given this evidence, I would predict that the GSP, and later IX, terminal field would demonstrate a similar phenomenon. I would also suggest that the overlap occurring between these two terminal fields would be extensive and occur in areas where the two terminal fields are densest, but that this overlap would not mature until postnatal synaptic stabilization occurs in response to peripheral stimuli. Such maturation might involve significant protracted paring back of initially exuberant terminals over protracted postnatal period. This protracted period is predicted based upon the lengthy anatomical and functional maturation of peripheral taste receptors in hamster.

In order to examine the plastic changes associated with this process, further research must be accomplished. First, a simultaneous labeling of all three primary taste afferents is crucial to accurately characterize the spatial organization and relationships of these terminal fields. Once this is achieved, examining the changes in terminal field volume and organization that occur during postnatal development could be accomplished. Considering this study has presented the first demonstrations of GSP terminal field and simultaneous IX/GSP terminal field as well as evidence of significant overlap with double labels, triple labels will be equally important to provide normative data for developmental studies that may provide rich evidence of activity-dependent changes in central gustatory organization.

Table 1. **Terminal Field Quantitative Morphometric Data**

	IX (N=6)	GSP (N=11)	IX/GSP (N=3)
Start Depth (μm)	183.3 ± 42.2	327.3 ± 31.9	283.3 ± 16.7
Dorsal-Ventral Extent (μm)	370.0 ± 46.7	322.4 ± 49.6	275.0 ± 32.5
Total Terminal Field Volume (μm^3)	63.3 ± 11.9 x 10^6	34.3 ± 4.6 x 10^6	27.7 ± 6.5 x 10^6
Dorsal Volume (%)	30.4 ± 2.8	22.2 ± 1.2	24.8 ± 5.0
Intermediate Volume (%)	47.5 ± 2.1	50.3 ± 3.2	49.7 ± 0.1
Ventral Volume (%)	22.1 ± 1.9	27.5 ± 3.8	25.4 ± 4.9

FIGURE 1: IX terminal field in NTS

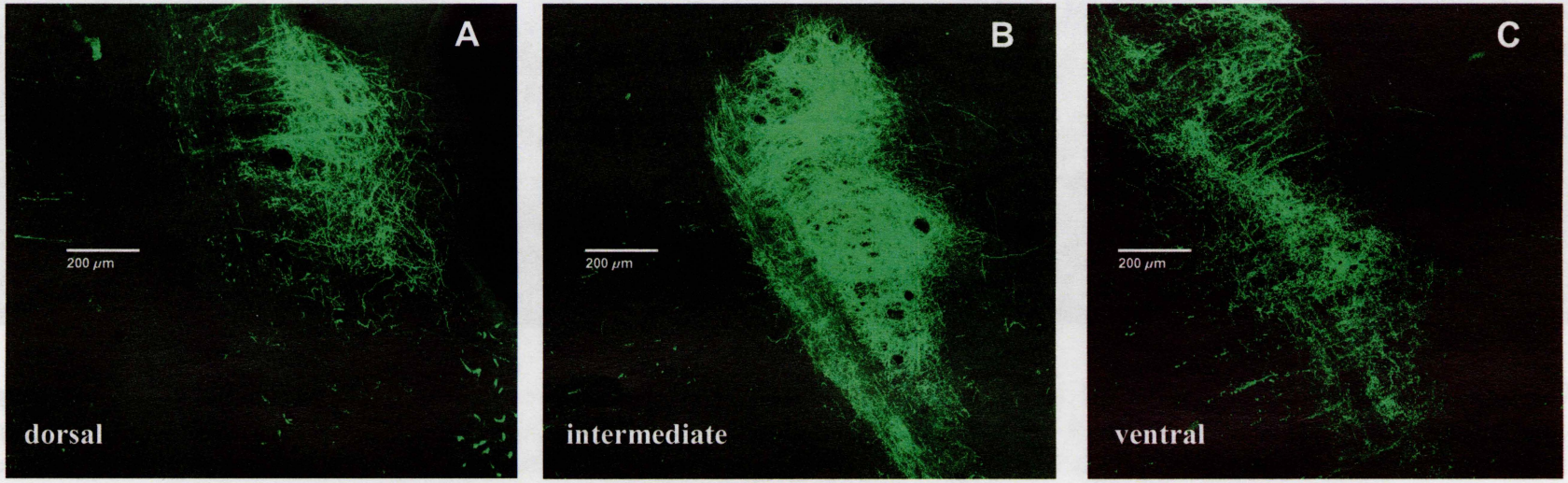

Figure 1: Horizontal sections of Cascade-Blue-dextran amine labeled IXth nerve terminal field. Terminal field of IX initially appeared ~250 μm (250 ± 39 μm) below the dorsal boundary of caudal NTS and extended ~315 μm (316 ± 24 μm) ventrally. Most IX nerve fibers exited the solitary tract and entered the NTS with a lateral trajectory, especially in the intermediate and ventral portions of the terminal field (B and C). More dorsally, fibers appeared to enter the NTS via a more rostral trajectory (A). Labeled IXth nerve terminal field was restricted to the rostral pole of NTS with the densest part of the field seen at intermediate levels in the dorsal-ventral extent of the field. In addition, below the dorsal most part of the field, two characteristic zones of heavy termination separated by a waist-like constriction were consistently observed (e.g., B and C).

FIGURE 2: GSP terminal field in NTS

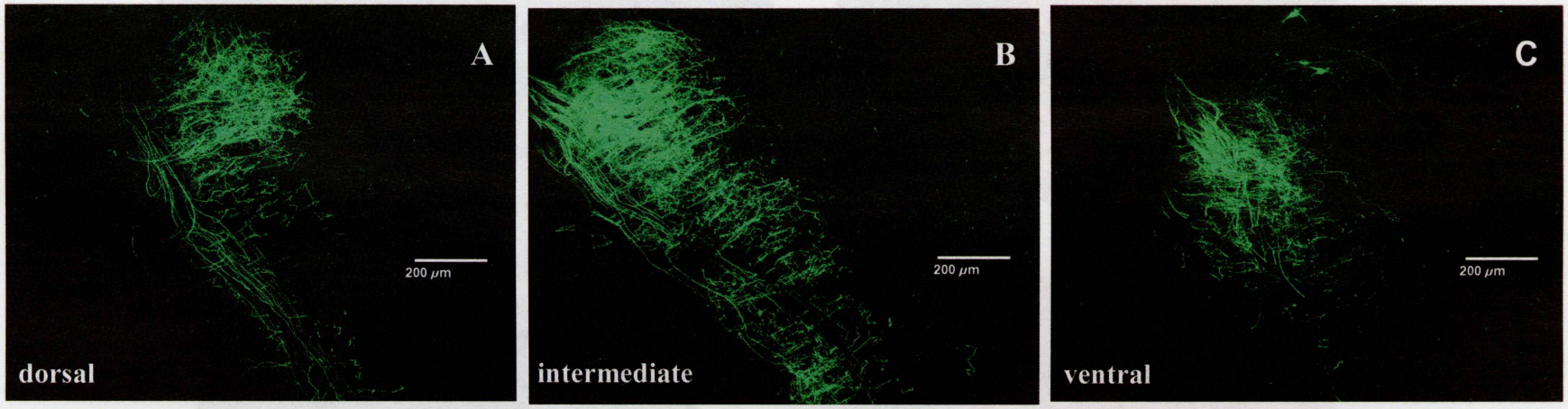

Figure 2: Horizontal sections of rhodamine green-dextran amine labeled GSP terminal field. GSP terminal field initially appeared ~270 μm (267 ± 33 μm) below the dorsal boundary of caudal NTS and extended ~375 μm (377 ± 46μm) ventrally. Most GSP fibers entered the NTS rostrally, especially in the intermediate and ventral portions of the terminal field (B and C). More dorsally, GSP fibers exited the solitary tract and entered the NTS with a more lateral trajectory (A). Labeled GSP terminal field was restricted to the rostral pole of NTS with the densest part of the field seen rostrolaterally, adjacent to the solitary tract (e.g., B). Retrogradely labeled secretomotor neurons were usually observed in the ventral most part of GSP terminal field (C). An interesting and consistent observation was the ramification of bundles of laterally-penetrating GSP fibers into tuft-like configurations, especially in the dorsal portions of the GSP terminal field (e.g., A).

FIGURE 3: Location of GSP and geniculate ganglion

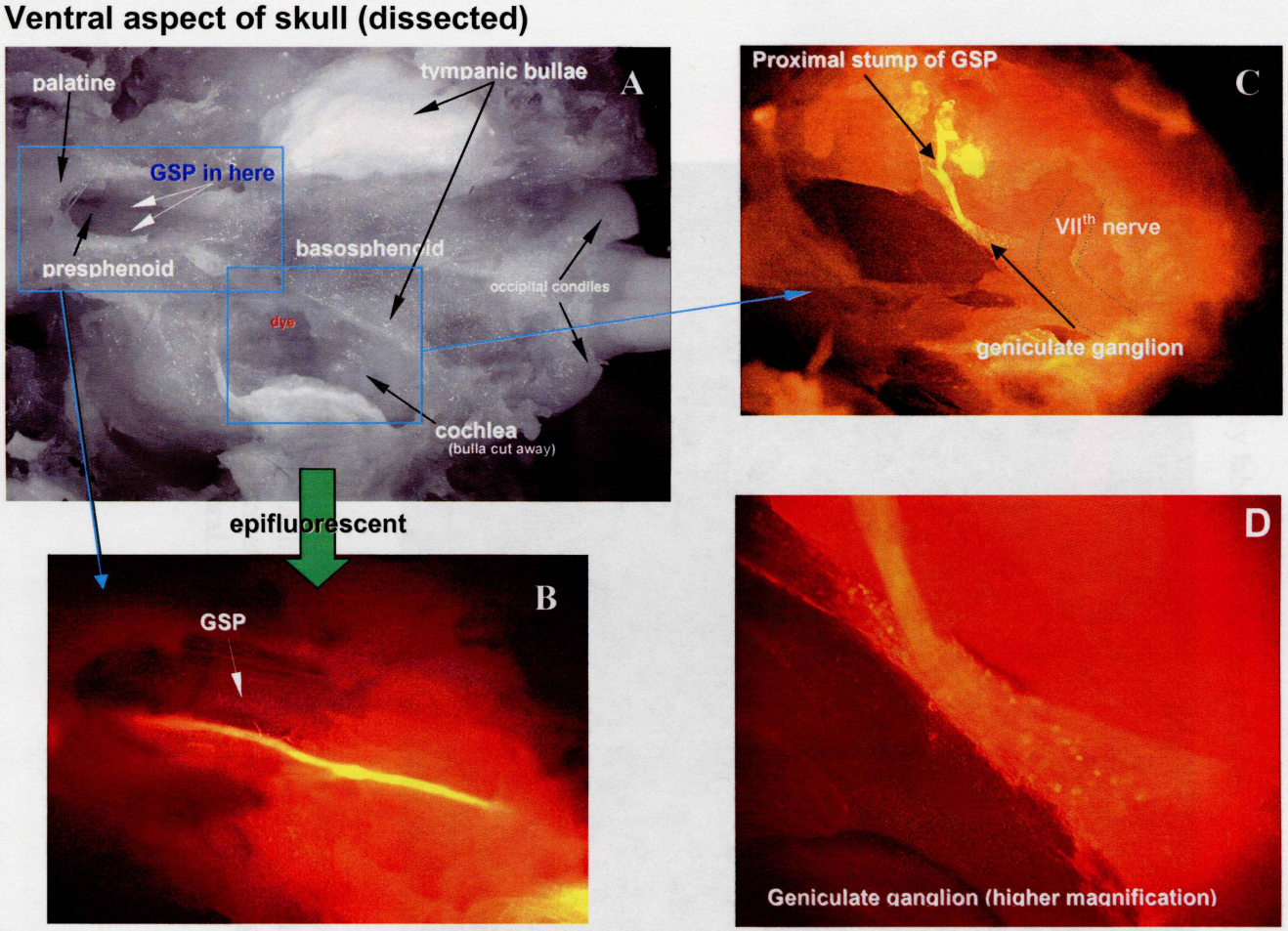

Figure 3: The GSP courses rostromedially under a plate in the basosphenoid bone, just anterior to the cochlea, and exits the tympanic bulla medially. The nerve then courses along the groove between the basosphenoid and bulla rostrally into the space defined by the presphenoid and palatine bones (A). Labeling of distal stump (B) is a good indication of a successful label. Cell bodies are easily seen under in situ epifluorescent illumination (C and D). Cell bodies of GSP axons are observed in the ganglion and distal nerve limb.

Figure 4: Micro-ruby labeled geniculate ganglion

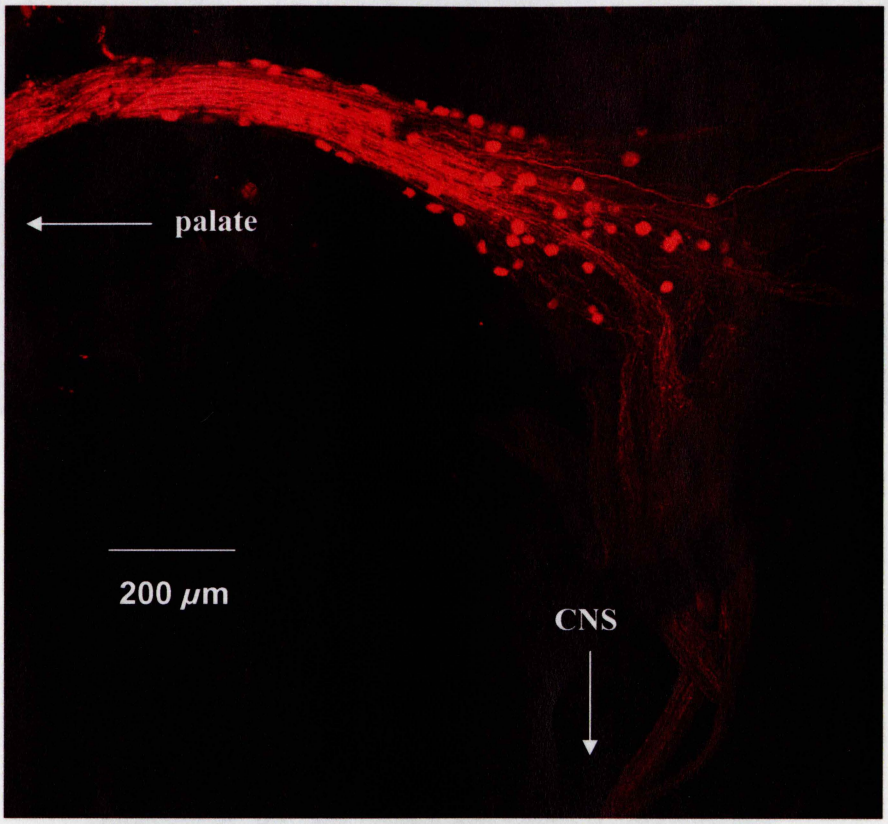

Figure 4: Micro-ruby labeled GSP axons penetrate the geniculate ganglion and then project via the facial nerve to the NTS. Cell bodies of GSP axons are found concentrated in the distal margin of the ganglion near the entry of the peripheral limb of the GSP.

Figure 5: Double labeled GPS and IX terminal field

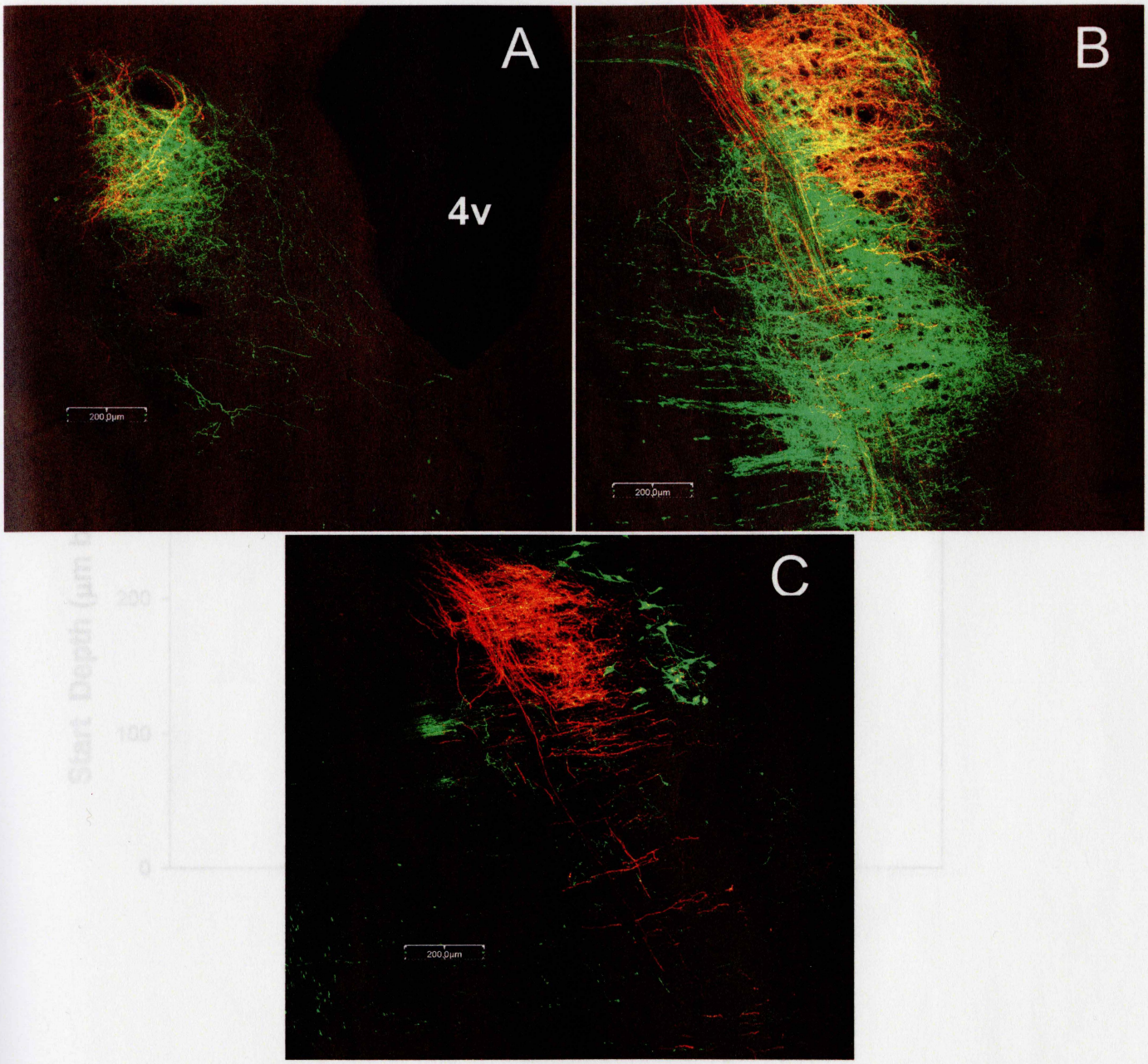

Figure 5: Horizontal sections of GSP and IX terminal fields labeled with micro-ruby (red) and Cascade Blue-dextran amine (green), respectively. IX terminal field appears ~25 μm more dorsal than GSP terminal field and the terminal fields intermingle extensively over a considerable dorsal-ventral extent (A and B). Overlap is especially prominent in the rostral-most parts of IX and GSP terminal fields. Parasympathetic neurons retrogradely labeled via IX appear more numerous than those associated with GSP, though some appear to be retrogradely labeled via both nerves (C).

Figure 6: Afferent Terminal Field Start Depth

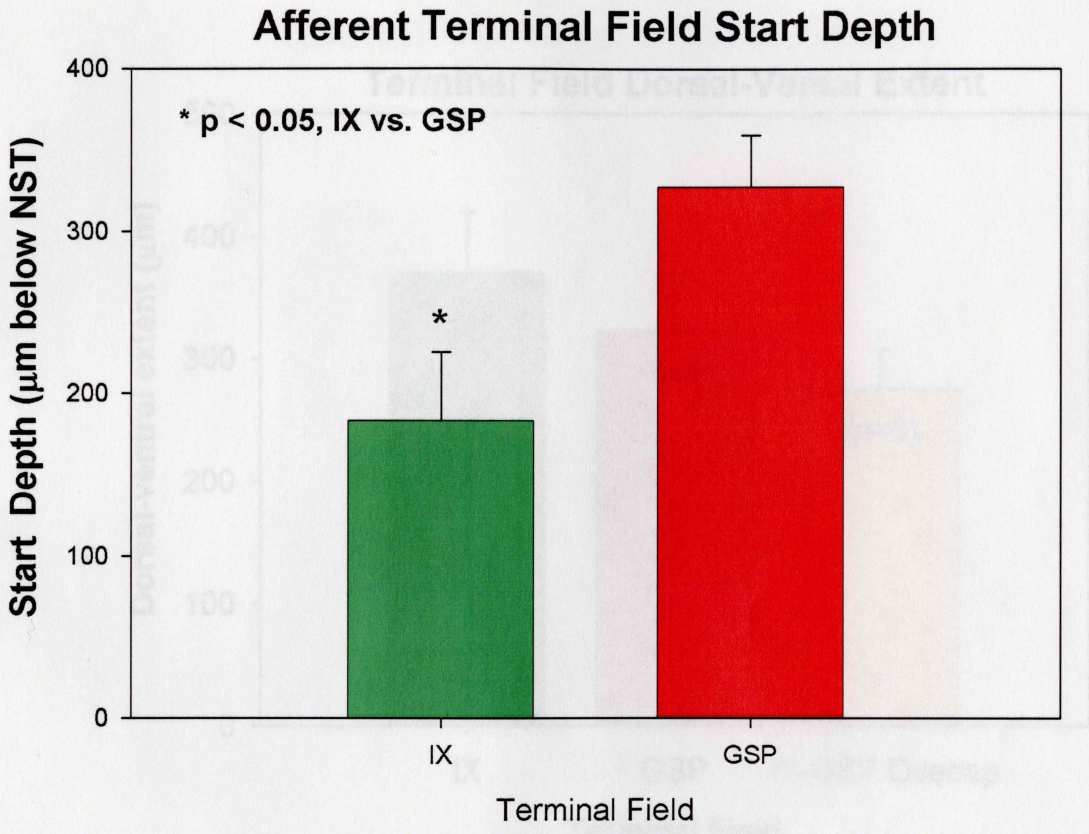

Figure 6. Afferent terminal field start depth. This graph provides a graphic demonstration of the relationship of the mean start depths for IX and GSP. Note that these two values are statistically different from one another.

Figure 7: Terminal Field Dorsal-Ventral Extent

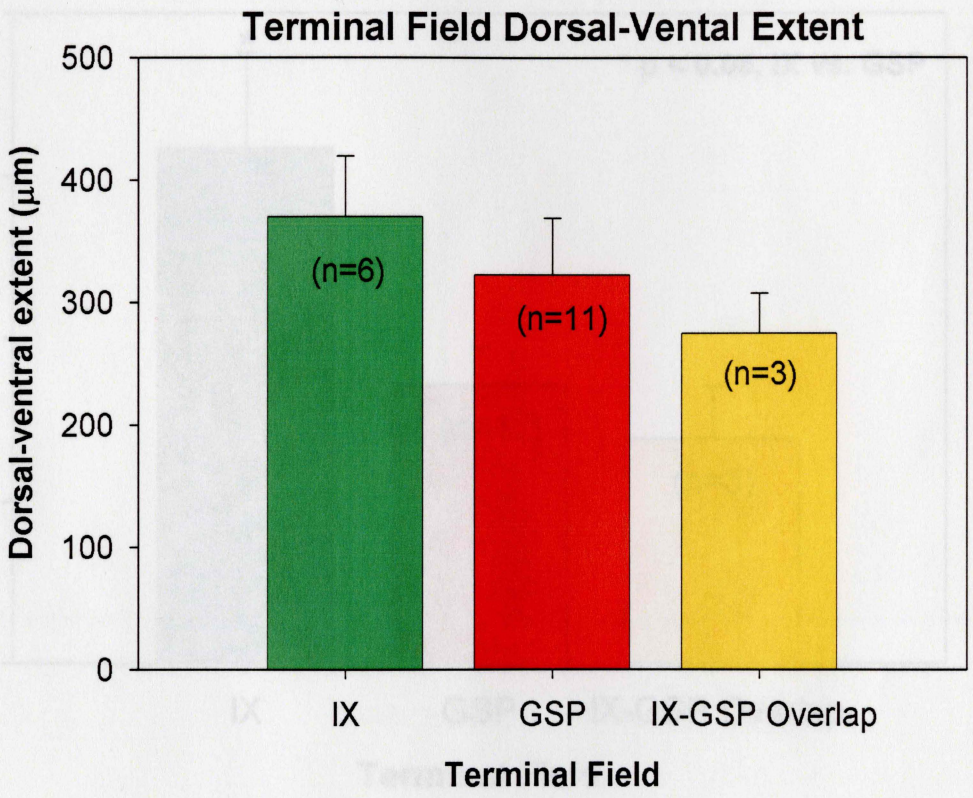

Figure 7. Terminal field dorsal-ventral extent. This figure provides a graphic demonstration of the relationship between the mean dorsal-ventral extent values for IX, GSP, and IX-GSP overlap terminal fields. Note that none of these values are statistically significant from one another.

Figure 8: Afferent Terminal Field Volumes

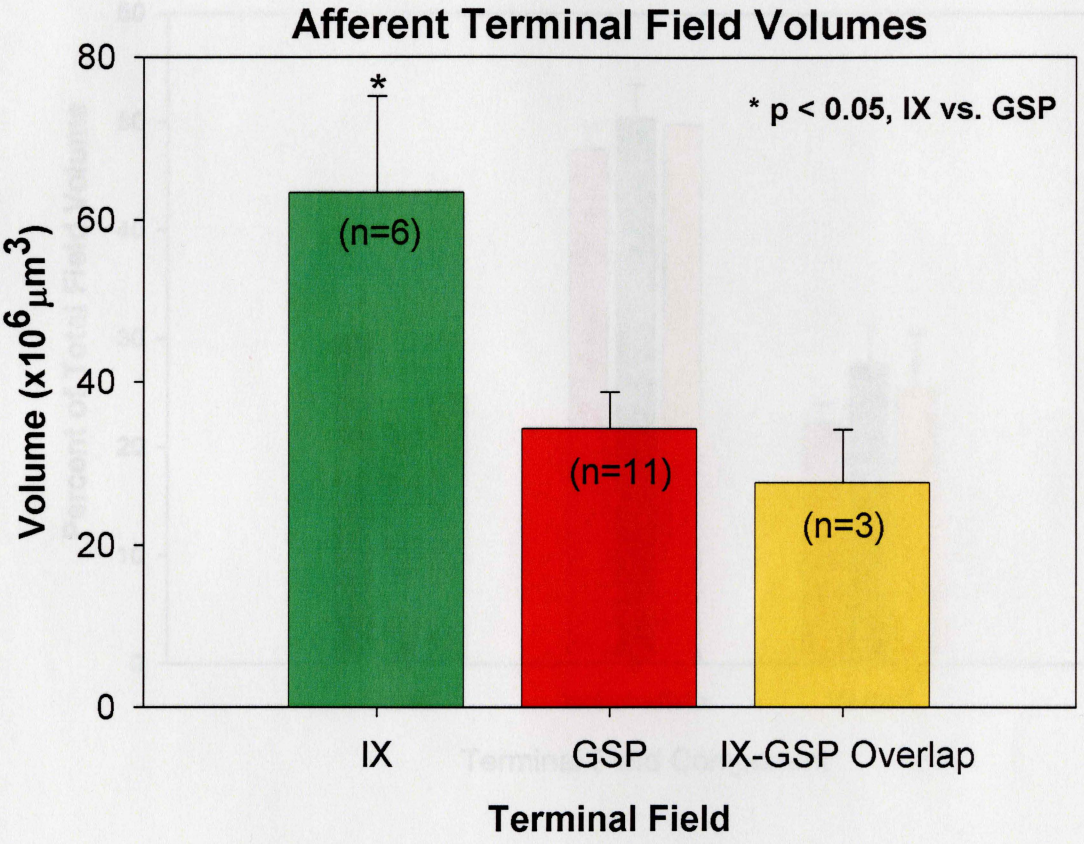

Figure 8. Afferent terminal field volumes. This figure provides a graphic representation of the total IX, GSP, and IX/GSP overlap terminal field volumes. Note that the IX terminal field volume is significantly larger than that of GSP.

Figure 9: GSP, IX, and GSP/IX Terminal Field Volume Distribution in NTS

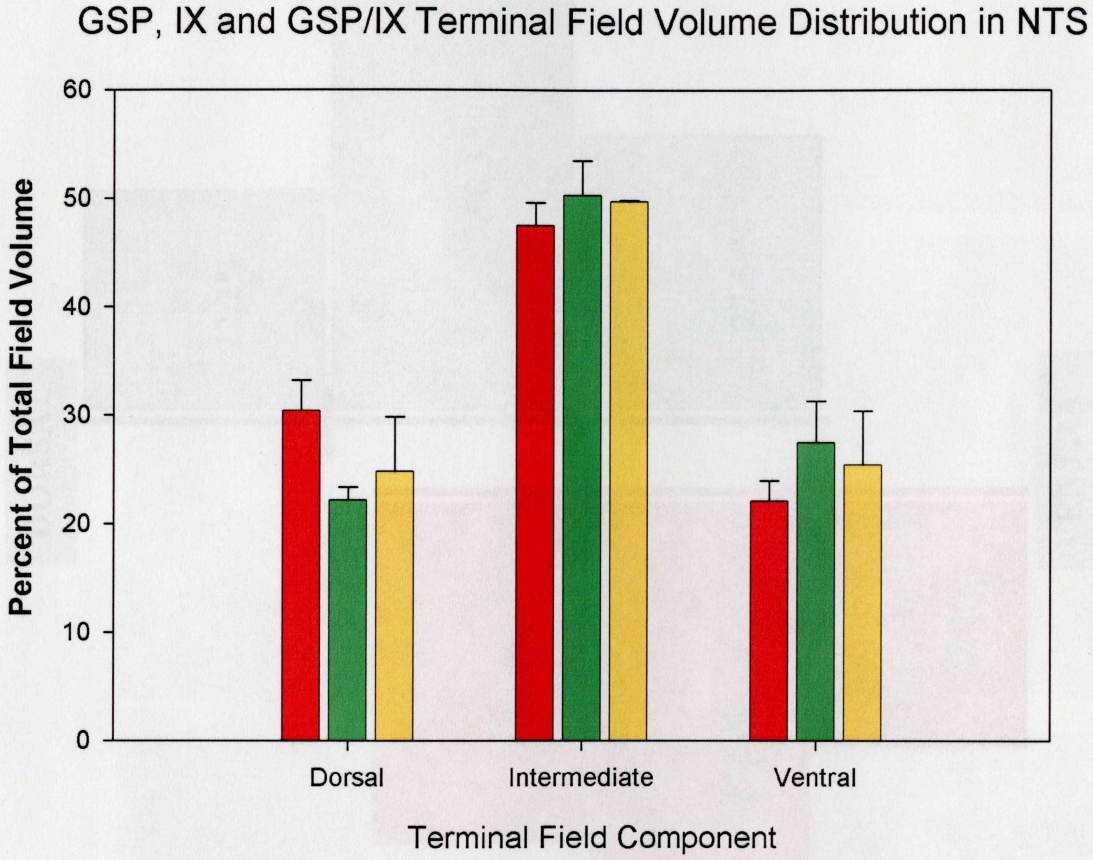

Figure 9. GSP, IX, and GSP/IX terminal field volume distribution in NTS. This figure provides a graphic representation of the relationship between the dorsal, intermediate, and ventral zones of the GSP (red), IX (green), and GSP/IX overlap (yellow) terminal fields.

Figure 10: Schematic Spatial and Volumetric Representation of GSP and IX Terminal Fields

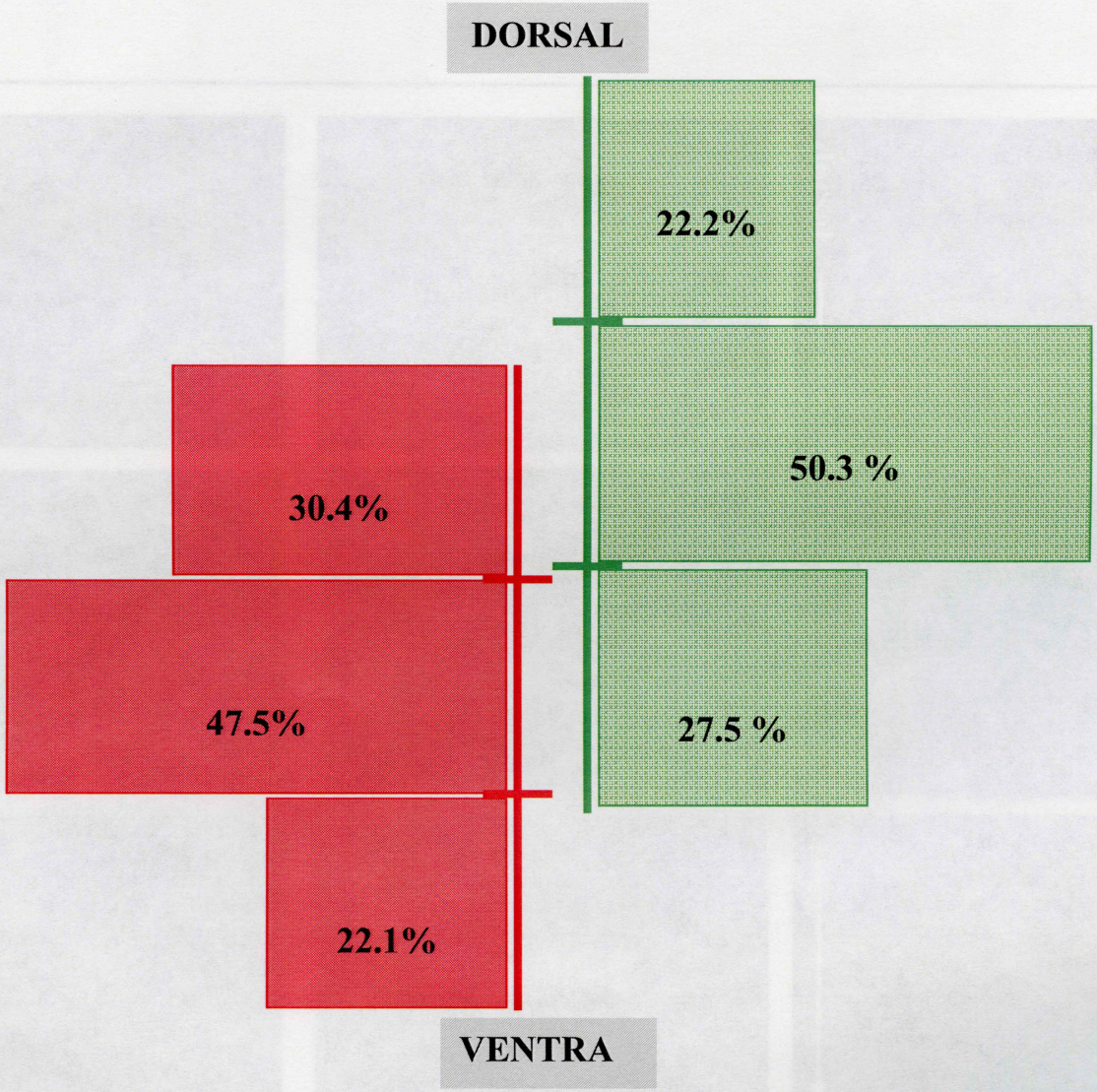

Figure 10: Each terminal field (GSP, red; IX, green) was divided into thirds, and the percentage of the total volume represented by the width of each third. The start depths and dorsal-ventral extents are scaled to demonstrate the spatial relationship between the two fields in the dorsal-ventral plane. This schematic allows for a prediction of where the greatest amount of overlap between the two fields would be found.

Figure 11: Example confocal serial optical sections through double-labeled a GSP/IX physical section

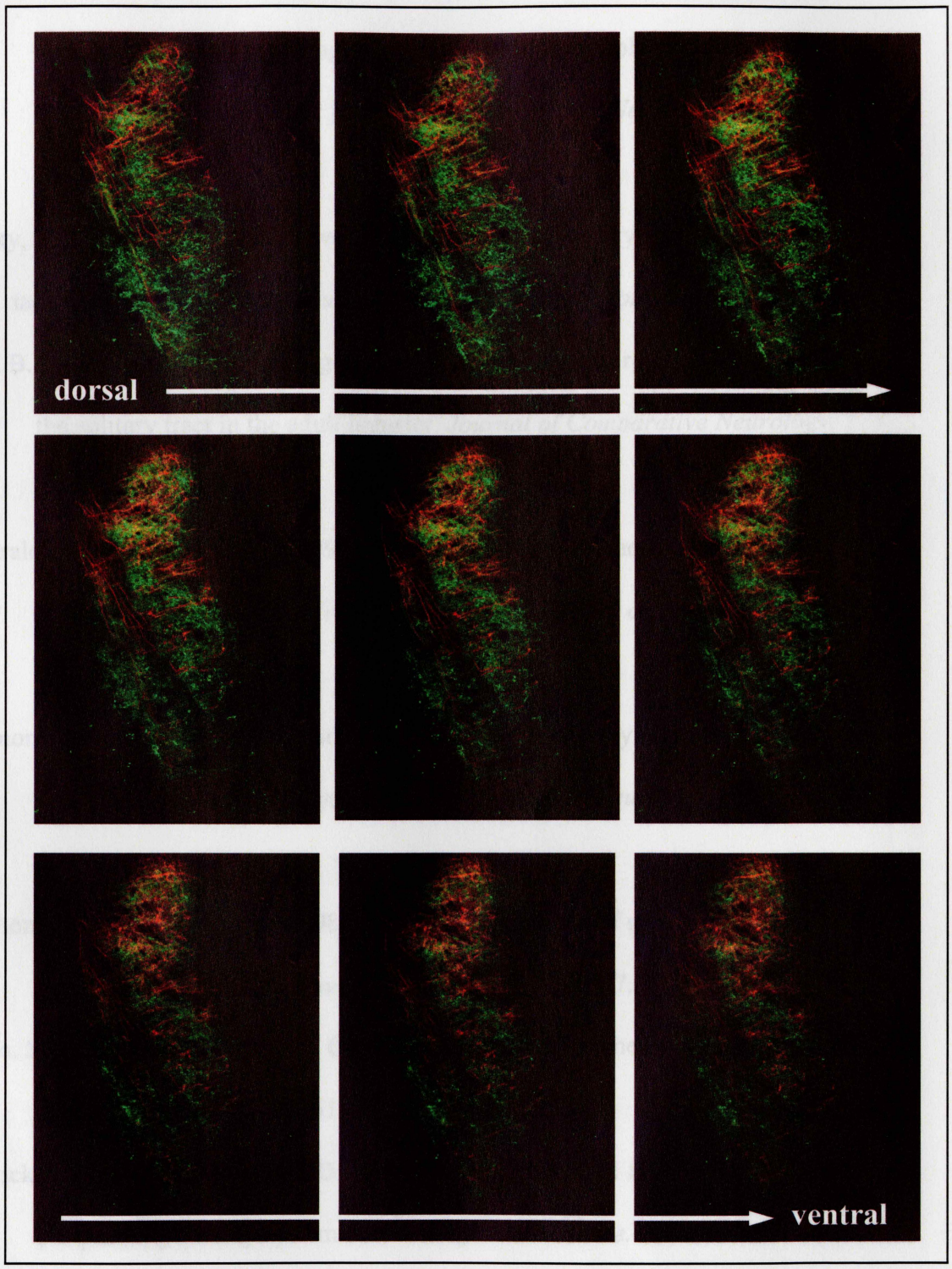

Figure 11: Serial 3 μm horizontal optical sections through GSP and IX terminal fields. This series of optical sections more clearly shows the prominent overlap of IX and GSP terminal fields in the rostral-most portion of IX field. While GSP field appeared over about the same rostral-caudal extent as IX, IX terminations are much denser caudally. Overlap of IX and GSP was far less pronounced caudally.

REFERENCES

Balice-Gordon, R. J., & Lichtman, J. W. (1993). In vivo observations of pre- and postsynaptic changes during the transition from multiple to single innervation at developing neuromuscular junctions. *The Journal of Neuroscience, 13*, 834-855.

Belecky, T. L. (1990). Postnatal development of palatal and laryngeal taste buds in the hamster. *Journal of Comparative Neurology. 293*(4), 646-654.

Davis, B. J., & Jang, T. (1988). A golgi analysis of the gustatory zone of the nucleus of the solitary tract in the adult hamster. *Journal of Comparative Neurology, 278,* 388-396.

Fitzgerald, M., & Jennings, E. (1999). The postnatal development of spinal sensory processing. *Proceedings from the National Academy of the Sciences, 96,* 7719-7722.

Hanamori, T., Miller, I. J. Jr, & Smith, D. V. (1988). Gustatory responsiveness of fibers in the hamster glossopharyngeal nerve. *Journal of Neurophysiology, 60,* 478-498.

Hamilton, R. B., & Norgren, R. (1984). Central projections of gustatory nerves in the rat. *Journal of Comparative Neurology, 222,* 560-577.

Harada, S., & Smith, D. V. (1992). Gustatory sensitivities of the hamster's soft palate. *Chemical Senses, 17*, 37-51.

Hendricks S.J., Sollars S.I., & Hill D.L. (2002). Injury-induced functional plasticity in the peripheral gustatory system. *Journal of Neuroscience. 22*(19), 8607-8613.

Hill, D.L. (1988). Development of chorda tympani nerve taste responses in the hamster.

Journal of Comparative Neurology, 268, 346-356.

Hubel, D. H., & Wiesel, T. N. (1970). The period of susceptibility to the physiological effects of unilateral eye closure in kittens. *Journal of Physiology (London), 206,* 419-436.

Hubel, D. H., & Wiesel, T. N. (1979). Brain mechanisms of vision. *Science America, 241,* 150-162.

Jacquin, M.F., Rhoades, R.W., & Klein, B.G. (1995). Structure-function relationships in rat brainstem subnucleus interpolaris. XI. Effects of chronic whisker trimming from birth.. *Journal of Comparative Neurology, 356*, 200-24

Kaas, J.H., & Collins, C.E. (2003). Anatomic and functional reorganization of somatosensory cortex in mature primates after peripheral nerve and spinal cord injury. *Advances in Neurology, 93,* 87-95.

Lasiter, P. S. (1992). Postnatal development of gustatory recipient zones within the nucleus of the solitary tract. *Brain Research Bulletin, 28,* 667-677.

Lasiter, P. S., & Diaz, J. (1992). Artificial rearing alters development of the nucleus of the solitary tract. *Brain Research Bulletin. 29,* 407-410.

Lasiter, P. S., & Kachele, D. L. (1990). Effects of early postnatal receptor damage on development of gustatory recipient zones within the nucleus of the solitary tract. *Brain Research: Developmental Brain Research, 55,* 57-77.

LeVay, S., Hubel, D.H., & Wiesel, T. N. (1980). The development of ocular dominance columns in normal and visually deprived monkeys. *Journal of Comparative Neurology, 19,* 1-51.

Mangold, J. E., & Hill, D. L. (2005). Postnatal development of gustatory nerve terminal

field development. [Abstract]. Association for Chemoreception Sciences, 27, 36.

Miller, I. J. Jr., & Smith, D. V. (1988). Proliferation of taste buds in the foliate and vallate papillae of postnatal hamsters. *Growth, Development , and Aging. 52*(3), 123-131..

Nakahara, H., Zhang, L. I., & Merzenich, M. M. (2004). Specialization of primary auditory cortex processing by sound exposure in the "critical period". *Proceedings from the National Academy of Sciences, 101,* 7170-7174.

Ojima, H., & Takayanagi, M. (2004). Cortical convergence from different frequency domains in the cat primary auditory cortex. *Neuroscience, 126,* 203-212.

Sollars, S.I., & Hill, D.L. (2000). Lack of functional and morphological susceptibility of the greater superficial petrosal nerve to developmental dietary sodium restriction. *Chemical Senses, 25*, 719-727.

Stewart, R. E., & DeSimone, J. A., Hill, D. L. (1997). New perspectives in a gustatory physiology: transduction, development, and plasticity. *American Journal of Physiology. 272*(1), C1-26.

St. John S.J., Garcea M., & Spector A.C. (2003). The time course of taste bud regeneration after glossopharyngeal or greater superficial petrosal nerve transection in rats. *Chemical Senses. 28*(1), 33-43.

Smith, D. V., & Shepard, G. M. (1999). Chemical senses: taste and olfaction. In Zigmond et al. (Eds.), *Fudamental Neuroscience* (pp. 722-723). San Diego, CA: Academic Press

Travers, S. P., & Norgren, R. (1995). Organization of orosensory responses in the

nucleus of the solitary tract of rat. *Journal of Neurophysiology, 73,* 2144-2162.

Whitehead, M.C. (1988). Neuronal architecture of the nucleus of the solitary tract in the hamster. *Journal of Comparative Neurology, 276,* 547-572.

Whitehead, M. C., & Frank, M. E. (1983). Anatomy of the gustatory system in the hamster: central projections of the chorda tympani and the lingual nerve. *Journal of Comparative Neurology, 270,* 378-395.

Whitehead, M. C., & Kachele, D. L. (1994). Development of fungiform papillae, taste buds, and their innervation in the hamster. *Journal of Comparative Neurology, 340,* 515-530.

Zigmond, M. J., Bloom, F. E., Landis, S. C., Roberts, J. L., & Squire, L. R. (Eds.) (1991). *Fundamental Neuroscience.* San Diego, CA: Academic Press.